Electrochemical behavior of Ni–P–SiC composite coatings: Effect of heat treatment and SiC particle incorporation

C. F. Malfatti*, J. Z. Ferreira, C. T. Oliveira, E. S. Rieder and J.-P. Bonino

This paper describes the effects of heat treatment and of SiC particle incorporation on the electrochemical behavior and physical structure of Ni–P (17 at% P) composite coatings. The deposits were obtained by electrodeposition with various contents of SiC particles in the plating bath and heat treated at 420 °C. The physical structure was investigated by inductively coupled plasma atomic emission spectrometry (ICP-AES), X-ray diffraction (XRD), and scanning electron microscopy (SEM – image analysis). The electrochemical behavior of the resultant composite coatings was determined by chronopotentiometry, electrochemical impedance spectroscopy, and potentiodynamic measurements in 0.6 M NaCl solution at pH 6. Heat treatment showed a positive effect on the electrochemical behavior of Ni–P coatings, shifting the open circuit potential toward less active potentials. The incorporation of SiC particles inhibited pit nucleation on the Ni–P composite coating, with or without post-heat treatment. However, heat treatment in the Ni–P–SiC seemed to induce cracks in the metallic matrix, initiating at the SiC particles, possibly caused by the contraction in the metallic matrix. The cracked structure promoted localized corrosion, while coatings without heat treatment resulted in a general and uniform corrosion.

1 Introduction

Ni–P alloys have been studied in the last few decades due to their characteristics concerning the effect of phosphorous content on its crystal structure [1, 2]. A transition from a crystalline to amorphous structure takes place progressively with phosphorous content in electrodeposited Ni–P coatings, resulting in amorphous structures when it exceeds 15 at% [2, 3]. Crystalline Ni–P structures can be obtained, though, by heat treatment above 350 °C [1], when crystallization of nickel and precipitation of nickel phosphide, Ni_3P, take place. It has been reported that the amorphous form, containing no grain boundaries and structure defects, results in coatings with outstanding mechanical and corrosion properties. Studies related to the electrochemical behavior of Ni–P alloys have been reported, particularly addressing the corrosion resistance of the amorphous structure in solutions containing high concentrations of Cl^-, NO_3^-, SO_4^{2-}, or SO_3^{2-} ions [4–7].

Ni–P alloys, however, present low hardness and consequently low wear resistance, restraining their application in industry. Studies to overcome this limitation have been performed. Structures with better wear resistance have been successfully achieved by the incorporation of ceramic particles in the metallic matrix, such as SiC, Al_2O_3, Cr_2O_3, and TiO_2 [8–16]. Also, heat treatment of Ni–P alloys has resulted in hardness of the order of 1000 Hv, the same as obtained for hard chromium [2, 12].

C. F. Malfatti
DEMET/PPGEM/Universidade Federal do Rio Grande do Sul, Av. Bento Gonçalves, 9500, Setor 4, Prédio 75, Sala 215, CEP 91501-970 – Porto Alegre/RS (Brazil)
E-mail: celia.malfatti@ufrgs.br

J. Z. Ferreira
DEMAT/PPGEM/Universidade Federal do Rio Grande do Sul, Av. Bento Gonçalves, 9500, Setor 4, Prédio 75, Sala 217, CEP 91501-970 – Porto Alegre/RS (Brazil)

C. T. Oliveira
PROPTEC/ICET/GEMA/Centro Universitário Feevale, RS 239, 2755, CEP 93352-000 – Novo Hamburgo/RS (Brazil)

E. S. Rieder
Post Graduation Program in Engineering, Universidade Luterana do Brasil, Av. Farroupilha, 8001, Prédio 4, Sala 57, CEP 92425-900 Canoas/RS (Brazil)

J.-P. Bonino
Institut Carnot – CIRIMAT, Unité Mixte de Recherche CNRS-UPS-INP (no. 5085), Université Paul Sabatier, Bât. 2R1, 118 route de Narbonne 31062 Toulouse (France)

These effects have encouraged studies and the development of new Ni–P coatings [4–7, 11, 17–21].

These composite coatings can be obtained by electrodeposition or autocatalytic (electroless) processes, the first being more attractive due to its characteristics and low cost. The electrodeposition process consists of incorporating particles in the metallic matrix from an electrolyte containing particles in suspension [22–28]. Parameters affecting coating formation and new formulations for industrial applications have been widely documented [20, 23, 29].

The utilization of these composite coatings by industry depends on good resistance to wear as well as good corrosion resistance. There are some documented studies on the tribological properties and the electrochemical behavior of Ni–P composite coatings [1, 2, 12, 30–33]. According to these papers, the corrosion resistance of Ni–P coatings can be optimized by the incorporation of particles in the deposits and it depends on factors such as the particle type, size and concentration, and process parameters. A remarkable improvement in the resistance to localized corrosion of Ni–SiC composite coatings was observed with alloys containing sub-micron SiC particles [28]. *Lampke* et al. [34] showed that the corrosion behavior of composite coatings can be improved by particles the size of 200 nm up to particles the size of microns. Further studies are required to correlate process conditions with the microstructure of the coatings and their electrochemical behavior in different environments.

This work aims at studying the effects of heat treatment and of the particle incorporation on the electrochemical behavior of Ni–P and Ni–P–SiC (17 at% P) composite coatings containing various amounts of embedded SiC particles, in 0.6 M NaCl.

2 Experimental

2.1 Materials and methods

Ni–P and Ni–P–SiC (17 at% P) composite coatings with varying amounts of incorporated SiC particles were obtained by electrodeposition. The plating bath consisted of $NiSO_4$ 50 g/L, $NiCl_2{\cdot}6H_2O$ 60 g/L, H_3PO_3 20 g/L, H_3PO_4 50 g/L, Na_2SO_4 50 g/L, containing 0, 40, 80, and 200 g/L of SiC particles (with a mean diameter of 600 nm [35]) in suspension, at pH 2. The substrate and counter-electrode were made of copper and nickel, respectively.

Electrodeposition was carried out at 0.1 A/cm^2 (which resulted in 50 μm thick coatings, measured by optical microscopy) in a thermostatic cell (140 mL) at 80 °C for 45 min, with static vertical electrodes. A stirring system was used to keep the particles in suspension and to induce its movement toward the cathode. After the process, the specimens were ultrasonically cleaned in deionized water for 2 min. and heat treated at 420 °C for 1 h in N_2 atmosphere.

The concentration of SiC embedded in the Ni–P matrix (vol%) was determined by inductively coupled plasma atomic emission spectrometry (ICP-AES), with an error of 2 wt%. The measurements were performed by the National Center for Scientific Research (CNRS) in Lyon, and they do not provide the information about the references used. The number of incorporated particles per unit area (particles/μm^2) was determined by image analysis using scanning electron microscope (SEM – JEOL JSM 6400). The crystalline state and thickness of the deposits were obtained by X-ray diffraction analysis (XRD), using Cu Kα ($\lambda = 1.5418$ Å) radiation in the Phillips X'Pert diffractometer, and by optical microscopy, respectively.

2.2 Electrochemical test conditions

Open circuit potential (OCP), electrochemical impedance spectroscopy (EIS) and potentiodynamic measurements were performed in 0.6 M NaCl solution (pH 6) using an EG&G PAR 273 potentiostat and a Solartron 1250 frequency response analyzer. The EIS measurements were carried out at the OCP using a perturbation of 10 mV amplitude signal and frequency range of 100 kHz to 10 MHz. The measurements were performed after the establishment of a reasonable steady state condition, which was safely achieved after 30 min of immersion. After 1200 h of immersion in the NaCl solution, the coatings were observed in the SEM. Potentiodynamic measurements were performed at 0.5 mV/s, from −400 to +200 mV. The analyses were carried out in a three-electrode cell, using a saturated calomel electrode as reference and platinum as counter-electrode, with the working electrode area of 0.64 cm^2.

3 Results and discussion

3.1 Coating process

The correlation between the amount of SiC in the coating, expressed in volume percent and number of incorporated particles per unit area (particles/μm^2), and the concentration of particles suspended in the solution is presented in Fig. 1. The volume of SiC particles (vol%) embedded in the metallic matrix increased with increasing particle concentration in the solution, reaching a saturation point at about 17 vol% under the conditions used. Saturation at this volume was also observed by other

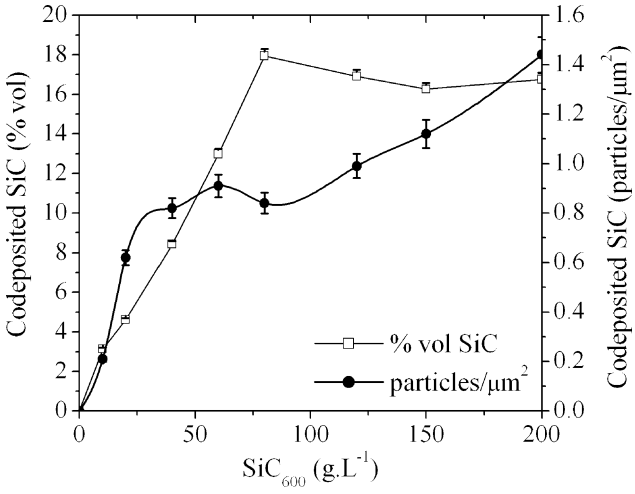

Figure 1. Effect of SiC particle incorporation in the coating as a function of SiC concentration in the electrolyte, expressed as volume percent (vol%) and particle number by unit area (particles/μm^2)

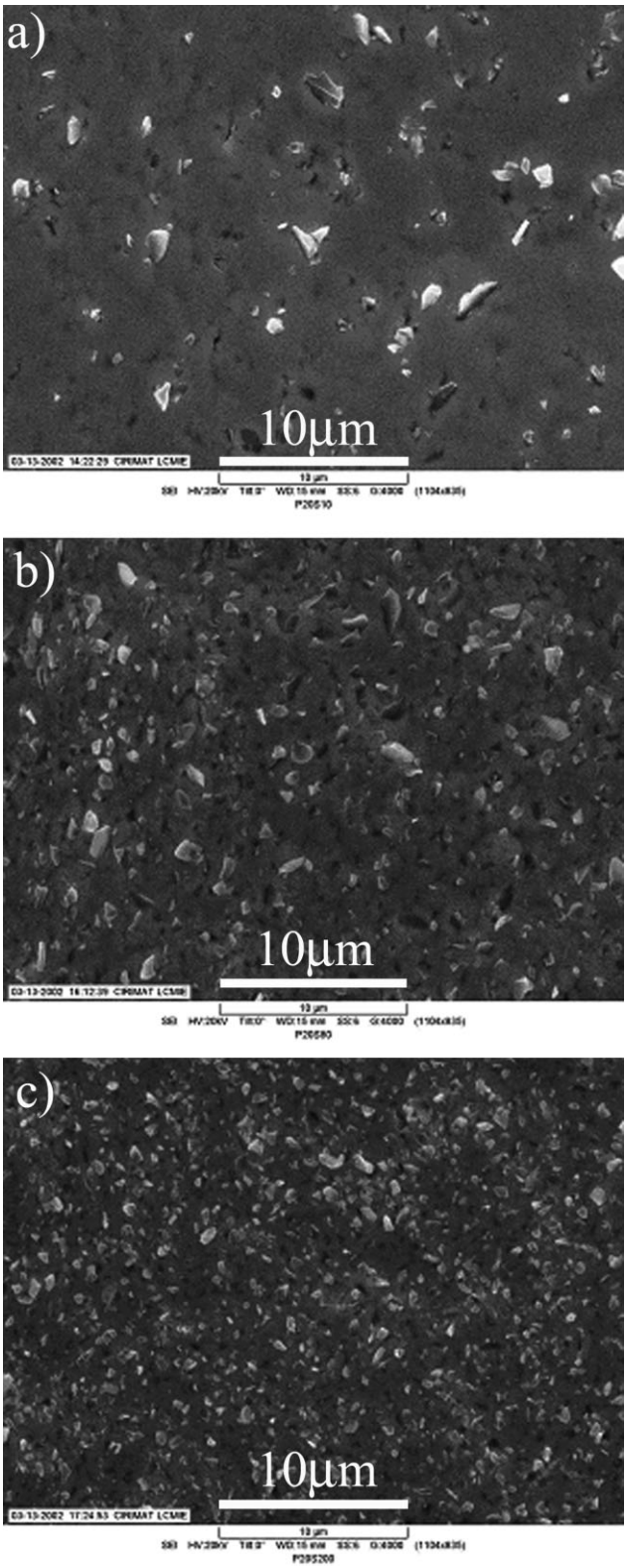

Figure 2. SEM micrographs of composite Ni–P–SiC coatings obtained from electrolytes with different concentrations of SiC particles: (a) 10 g/L; (b) 80 g/L; and (c) 200 g/L

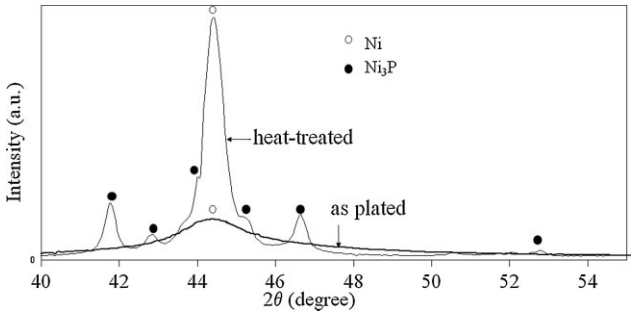

Figure 3. XRD patterns of Ni–P coatings: as plated and after heat treatment at 420 °C, for 1 h in N_2 atmosphere

authors [10]. However, the number of particles in the coating, showed no saturation under these conditions. The increase of particles concentration in the electroplating bath induced a selective phenomenon, promoting smaller particle embedded in the coating (Fig. 2a–c). This phenomenon, also observed by other authors in similar systems [11, 20, 25, 35–37], may be based upon the probability of mechanical interaction between the cathode and the suspended particles. The particle is completely incorporated into the metallic matrix only when the deposit reaches a certain thickness, so that the ejection, caused by the arriving particles, is restrained. The time required for complete particle incorporation is, therefore, a size function, i.e., bigger particles need longer periods for their complete incorporation into the metallic matrix [25]. The incorporation of particles must not affect phosphorous content in the deposit, which remained constant at about 17 at%.

Heat treatment at 420 °C for 1 h in N_2 atmosphere resulted in the crystallization of nickel followed by precipitation of nickel phosphide, Ni_3P ($Ni \rightarrow Ni_{(cfc)} + Ni_3P$), as shown by the XRD measurements results in Fig. 3. The structure went from amorphous (as-plated) to crystalline with thermal treatment. Studies on similar systems concluded [1, 38–40] that crystalline alloys are denser than microcrystallized and amorphous Ni–P alloys with the same chemical composition, and that the transition from amorphous to crystalline structure is accompanied by a volume contraction. This is in agreement with the

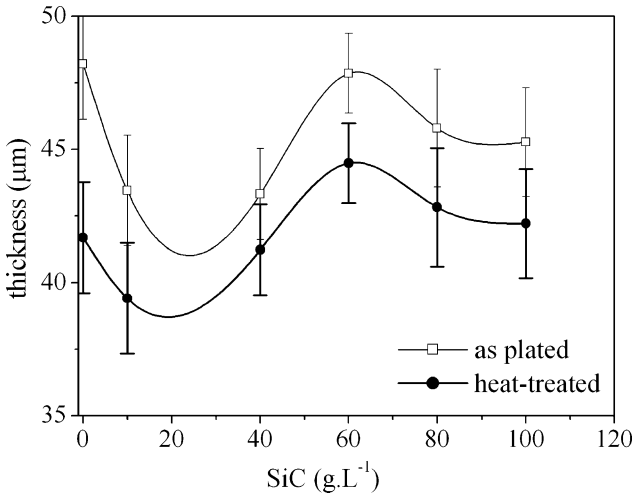

Figure 4. Effect of heat treatment on the coating thickness for various SiC particles contents in the electrolyte

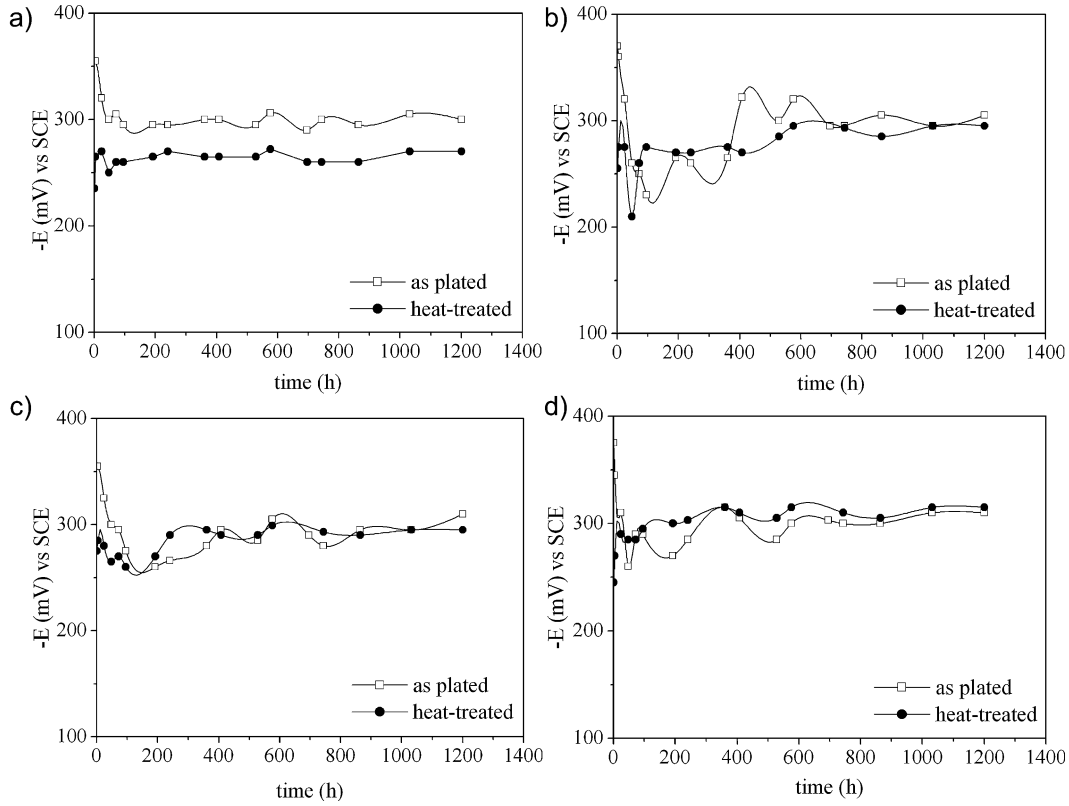

Figure 5. Open circuit potential *versus* time of immersion in 0.6 M NaCl, pH 6: (a) Ni–P; (b) Ni–P–SiC40; (c) Ni–P–SiC80; and (d) Ni–P–SiC200

observations for this system. The coatings suffered about 5% reduction in thickness with thermal treatment, as shown by the results of Fig. 4. This structural change and associated contraction, may influence cohesion between the SiC particles and the metallic matrix and, therefore, affect properties such as corrosion resistance.

3.2 Open circuit potential

Open circuit potential measurements with time (Fig. 5a) showed that thermal treatment of Ni–P coatings (without particles) displaced the OCP toward less active values compared to the as-plated specimens. This behavior was also observed by other authors [14, 18]. Comparing specimens during the first 100 h of immersion, a sharp drop in potential was observed on the as-plated specimens, which was not observed on specimens subjected to thermal treatment. The potential drop may be due to a film formed rapidly on the as-plated specimen in the first couple of hours of immersion in NaCl [8]. After this period, the OCP became stable for the entire period of immersion (1200 h). The heat treated specimens presented a steady potential during the whole period.

The as-plated Ni–P–SiC composite coatings also exhibited a potential drop in the first 100 h in the solution, becoming stable thereafter, independent of particle concentration in the metallic matrix (Fig. 5b–d). Heat treatment also caused the shift of the OCP to less active values in the first 100 h. After this period of time, it showed similar behavior as that of the specimens without thermal treatment, i.e., with a stable OCP.

3.3 Electrochemical impedance spectroscopy and potentiodynamic measurements

The electrochemical impedance results exhibited one time constant and the fitting parameters were equivalent to the circuit presented in Fig. 6, where R_s is the solution resistance, R_p the polarization resistance, and C_{dl} the double layer capacitance. The results are presented using Nyquist diagrams, Figs. 7 and 8. The spectra obtained for Ni–P and Ni–P–SiC coatings without thermal treatment in the first hour of immersion in 0.6 M NaCl, pH 6, showed very similar values of polarization resistance (40–45 $\Omega\,cm^2$), Fig. 7a. The same behavior was observed for the heat treated specimens (Fig. 7b), having in this case polarization resistance of the order of 20 $k\Omega\,cm^2$.

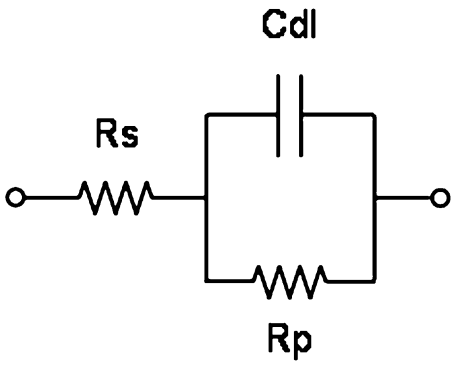

Figure 6. Equivalent circuit, where R_s is the solution resistance, R_p the polarization resistance, and C_{dl} the double layer capacitance

After 1200 h of immersion, while the as-plated Ni–P coatings (without particles) showed polarization resistance of the order of 100 kΩ cm^2 (Fig. 8a), the heat treated specimens exhibited 13 kΩ cm^2 (Fig. 8b). Other authors [7] have also observed, by impedance studies, higher polarization resistance for the non-treated Ni–P alloys compared to the heat treated specimens and attributed this effect to the crystal structure of the coating. Specimens without thermal treatment are amorphous and are supposed to exhibit better corrosion resistance. Nevertheless, the resistance values for the as-plated Ni–P coatings oscillated with time of immersion in NaCl solution, indicating that this system is less stable than the others (Fig. 9a). Pitting corrosion was observed, by SEM micrographs, on the as-plated Ni–P coatings (Fig. 10a and b) and evidenced by the potentiodynamic curve (Fig. 11). A typical passivity breakdown took place at around 70 mV. This behavior was not observed on the heat treated specimens, Figs. 10c and 11, which presented low current densities in the potential range measured. This evidence indicates that the higher R_p observed on the as-plated Ni–P coatings are not associated with a better corrosion resistance, but with some other phenomenon occurring during the attack. According to some authors [41, 42], Ni–P alloys can exhibit Ni selective dissolution, and the formation of a pseudopassivating unstable layer of $Ni_3(PO_4)_2$, which could be the case in this system.

For other coatings, except for the as-plated Ni–P, the R_p values, with or without heat treatment, were very unstable up to 100 h of immersion (Fig. 9a and b), in the same manner as observed for the OCP. After this time, a dark grey film formed on the surface and more stable values of polarization resistance were

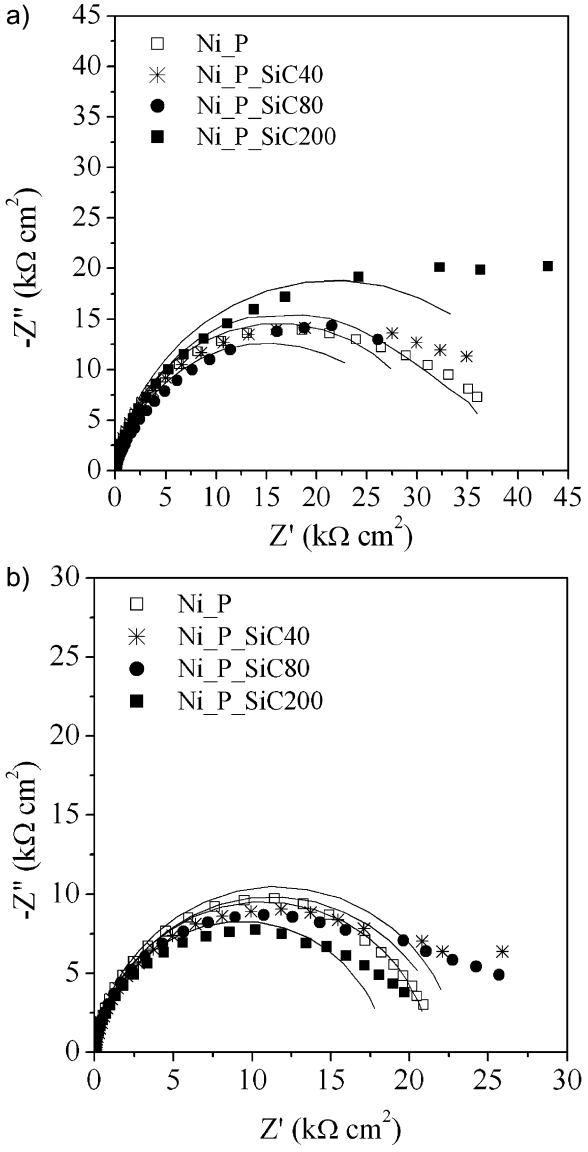

Figure 7. Nyquist plots for Ni–P, Ni–P–SiC40, Ni–P–SiC80, and Ni–P–SiC200 coatings at the OCP, after immersion in 0.6 M NaCl, pH 6, for 1 h: (a) as-plated and (b) heat-treated

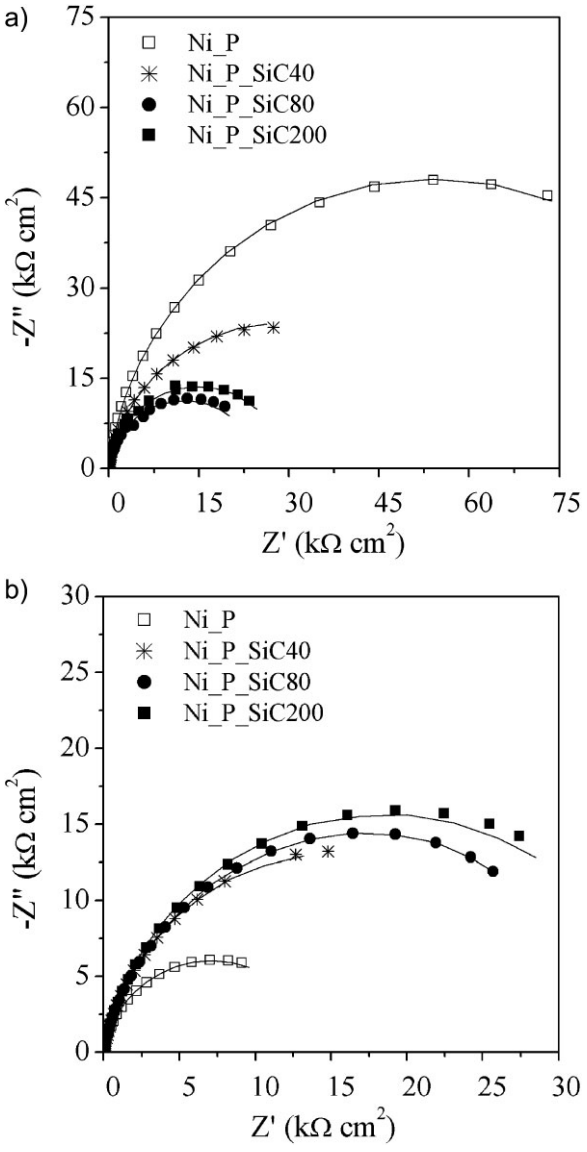

Figure 8. Nyquist plots for Ni–P, Ni–P–SiC40, Ni–P–SiC80, and Ni–P–SiC200 coatings at the OCP, after immersion in 0.6 M NaCl for 1200 h: (a) as-plated and (b) heat-treated

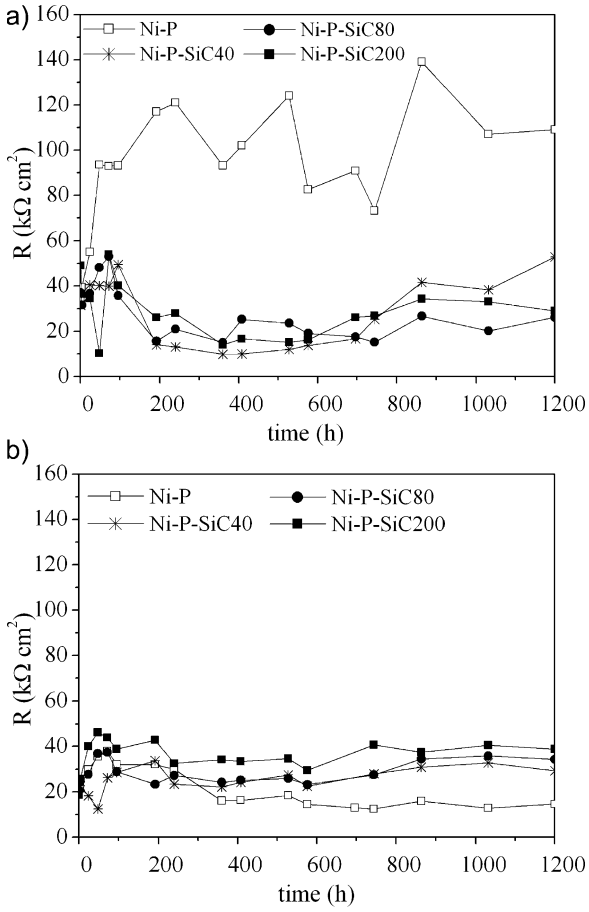

Figure 9. Polarization resistance *versus* time of immersion in 0.6 M NaCl, pH 6 for Ni–P and Ni–P–SiC600 coatings: (a) as-plated and (b) heat-treated

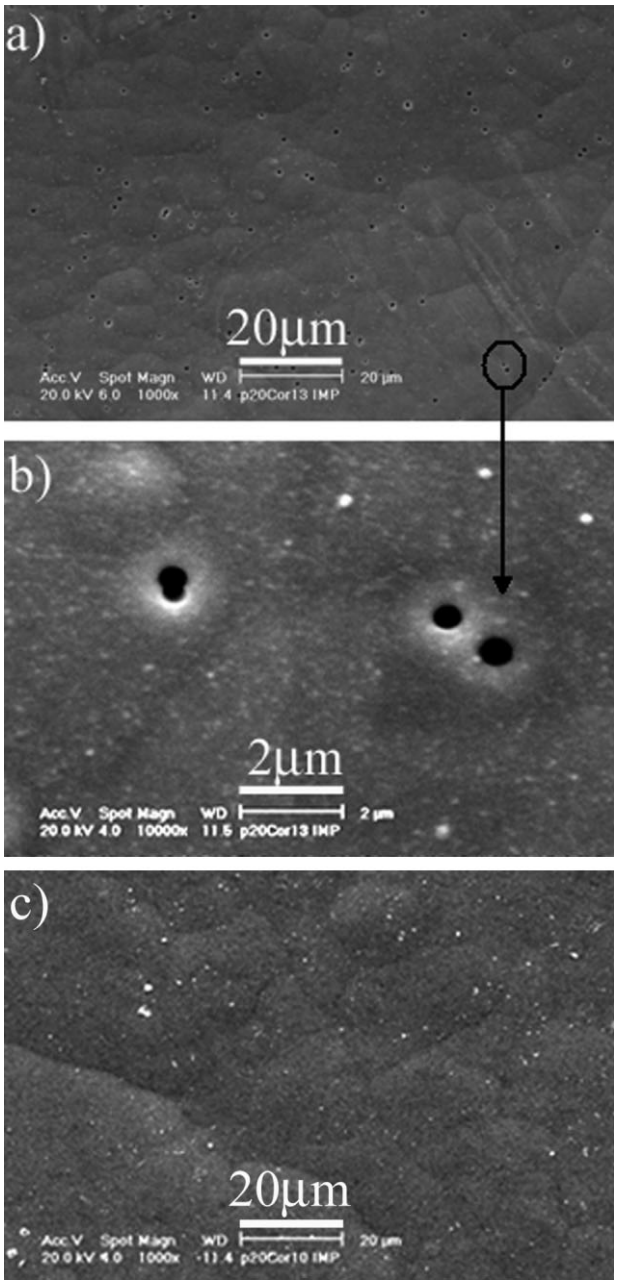

Figure 10. SEM micrographs of a Ni–P coating after 1200 h immersed in 0.6 M NaCl, pH 6: (a) as-plated; (b) as-plated (higher magnification); and (c) heat-treated

obtained. Similar results were documented by *Królikowski* et al. [43] and *Diegle* et al. [5].

According to *Schenzel* and *Kreye* [14], Ni–P alloys treated at 650 °C for 20 h exhibited coalescence of nickel phosphide, resulting in a continuous Ni_3P layer with isolated areas containing nickel crystals, generating an alloy very resistant to pitting. *Gillot* et al. [44] showed that Ni–P alloys, heat treated between 600 and 800 °C for 5 h, produced a phosphide layer, making the alloy more resistant to corrosion at high temperatures. The resistance to localized corrosion is, however, limited in chloride media, as already mentioned in a previous report [35].

The incorporation of SiC particles in the Ni–P coatings affected the polarization resistance (Fig. 8a and b). Lower R_p values were obtained for the as-plated Ni–P–SiC specimens, and higher values for heat treated Ni–P–SiC, compared to the Ni–P coatings. Higher values, with increasing SiC content in the coating, were also obtained by other authors [28, 45]. Variations in electrochemical activity of Ni–P–SiC coatings may be related to the surface area effectively exposed to the electrolyte, which is the Ni–P area, once SiC particles are electrochemically inactive. Structural changes in the Ni–P matrix itself with the incorporation of particles are less likely.

While thermal treatment had an important effect on the polarization resistance, the amount of incorporated particle seemed to have no influence on its value. The polarization resistance for Ni–P–SiC coatings showed no variation according to its particle content (40, 80, and 200 g/L SiC in solution), exhibiting very similar values, 20–50 kΩ cm^2 (Fig. 9a and b).

The as-plated Ni–P–SiC coating, immersed in NaCl solution for 1200 h, exhibited general corrosion on the surface of the Ni–P matrix (Fig. 12a), while the heat treated Ni–P–SiC specimens showed localized corrosion at the interface between Ni–P and SiC particles (Fig. 12b), exhibiting low peak currents at around

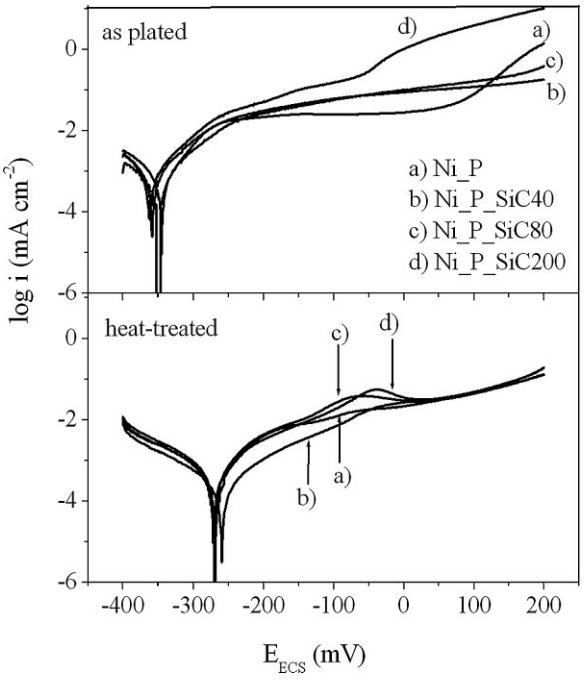

Figure 11. Potentiodynamic curves at 0.5 mV/s, of as-plated and heat-treated samples immersed in 0.6 M NaCl, pH 6

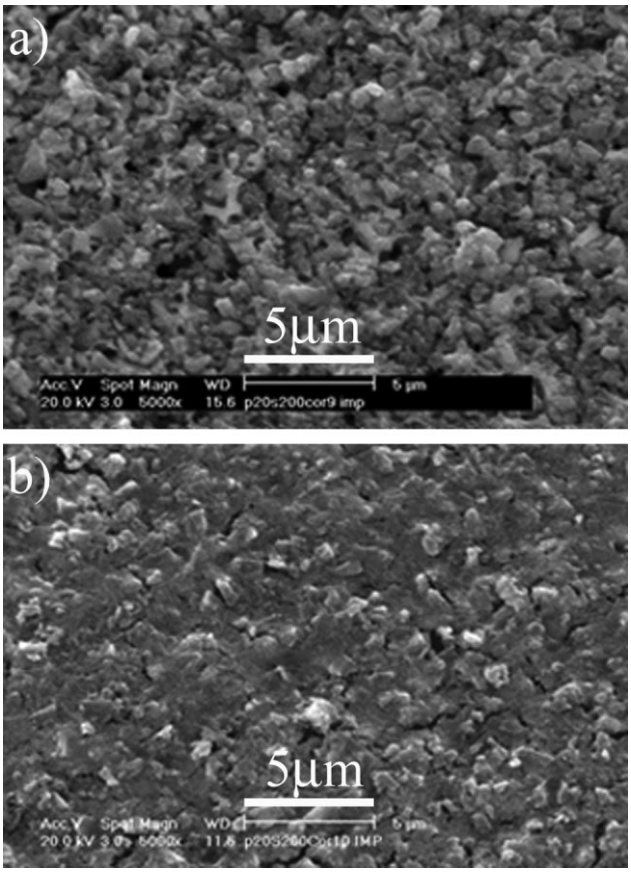

Figure 12. SEM micrographs of a Ni–P–SiC200 coating after 1200 h immersed in 0.6 M NaCl, pH 6: (a) as-plated and (b) heat-treated

−60 mV on the potentiodynamic curves (Fig. 11). With thermal treatment, structural change and contraction may occur, as presented above (Fig. 3). The contraction, which cannot be accommodated by the embedded particles, can result in fissures initiating at the particles, contributing to localized corrosion at the interface Ni–P–SiC.

4 Conclusions

The results obtained in this work showed that thermal treatment causes microstructural changes in the Ni–P matrix, going from amorphous to crystalline, followed by a slight contraction in the metallic matrix (5%). These changes impact the electrochemical behavior of Ni–P coatings. Heat treatment at 420 °C for 1 h shifts the OCP toward less active values, preventing pit formation.

The concentration of particles in the solution affects the particle size incorporated in the coating. The higher the concentration in solution, the smaller the particle embedded in the coating. Phosphorous content in the deposit is not affected by the embedded particles, and remained constant at about 17%.

The higher R_p observed on the as-plated Ni–P (without particles) was not related to a better corrosion resistance but with some other phenomenon occurring during the attack.

The incorporation of particles in the coating results in higher polarization resistance, compared to the coatings containing only the metallic matrix (Ni–P), for heat treated specimens. Heat-treated Ni–P–SiC composite coatings, despite particle concentration or particle size, exhibit higher polarization resistance than the Ni–P coatings. The lower electrochemical activity has been associated with the smaller active surface area established by the non-conductive SiC particles.

Acknowledgements: This work was supported by CAPES, CNPq, and CNRS.

5 References

[1] J.-P. Bonino, S. Bruet-Hotellaz, C. Bories, P. Pouderoux, A. Rousset, *J. Appl. Electrochem.* **1997**, *27*, 1193.
[2] S. Vaillant, *PhD Thesis*, Université Paul Sabatier, Toulouse, France **2002**.
[3] B. Färber, E. Cadel, A. Menand, G. Schmitz, R. Kirchheim, *Acta Mater.* **2000**, *48*, 789.
[4] M. Ratzker, D. S. Lashmore, K. W. Pratt, *Plat. Surf. Finish.* **1986**, *73*, 74.
[5] R. B. Diegle, N. R. Sorensen, G. C. Nelson, *J. Electrochem. Soc.* **1986**, *133*, 1769.
[6] K. T. Ziehlke, W. S. Dritt, C. H. Mahoney, *Met. Prog.* **1960**, *February*, 84.
[7] M. M. V. Parente, O. R. Mattos, S. L. Díaz, P. Lima, F. J. Neto, Miranda. Fabri, *J. Appl. Electrochem.* **2001**, *31*, 677.
[8] O. Berkh, S. Eskin, J. Zahavi, *Met. Finish.* **1996**, *94*, 35.
[9] Y. Li, *Plat. Surf. Finish.* **1997**, *84*, 77.
[10] S. Shawki, Z. A. Hamid, *Anti-Corr. Meth. Mater.* **1997**, *44*, 178.

[11] A. Grosjean, *PhD Thesis*, Université de Besançon, Besançon, France **1998**, p. 215.
[12] S. Vaillant, L. Datas, J.-P. Bonino, *Matér. Tech.* **2001**, *89*, 47.
[13] P. Lima Neto, F. J. B. Rabelo, A. M. M. M. Adam, L. A. Avaca, E. R. Gonzalez, *Interfinish* **1988**, *92*, 385.
[14] H. G. Schenzel, H. Kreye, *Plat. Surf. Finish.* **1990**, *77*, 50.
[15] I. Apachitei, F. D. Tichelaar, J. Duszczyk, L. Katgerman, *Surf. Coat. Technol.* **2002**, *149*, 263.
[16] J. Ma, Y. Shi, J. Di, Z. Yao, H. Liu, *Mater. Corros.* **2009**, *60*, 274.
[17] M. Verelst, *PhD Thesis*, Université de Toulouse 3, Toulouse, France **1991**.
[18] A. Lavanant, *PhD Thesis*, Université de Paris 06, Paris, France **1991**.
[19] M. Verelst, J. P. Bonino, M. Brieu, A. Rousset, *Mater. Sci. Eng.* **1995**, *A 191*, 165.
[20] I. Garcia, J. Fransaer, J.-P. Celis, *Surf. Coat. Technol.* **2001**, *148*, 171.
[21] L. Benea, P. L. Bonora, A. Borello, S. Martelli, *Wear* **2001**, *249*, 995.
[22] J. W. Graydon, D. W. Kirk, *J. Electrochem. Soc.* **1990**, *137*, 2061.
[23] A. Hovestad, L. J. J. Janssen, *J. Appl. Electrochem.* **1995**, *25*, 519.
[24] M. J. Bhagwat, J. P. Celis, J. R. Ross, *Trans. Inst. Met. Finish.* **1983**, *61*, 72.
[25] J. P. Celis, J. R. Roos, C. A. Buelens, *J. Electrochem. Soc.* **1987**, *134*, 1402.
[26] N. Guglielmi, *J. Electrochem. Soc.* **1972**, *119*, 1009.
[27] J. Fransaer, J. P. Celis, J. R. Roos, *J. Electrochem. Soc.* **1992**, *139*, 413.
[28] I. Garcia, A. Conde, G. Langelaan, J. Fransaer, J. P. Celis, *Corros. Sci.* **2003**, *45*, 1173.
[29] J. A. Ortega, J. Font, presented at *Congres de Depots Metalliques avec Particules*, Saint-Etienne/France, Anais Saint-Etienne, França **1996**.
[30] I. R. Aslanyan, J.-P. Bonino, J.-P. Celis, *Surf. Coat. Technol.* **2006**, *200*, 2909.
[31] F. Bratu, L. Benea, J.-P. Celis, *Surf. Coat. Technol.* **2007**, *201*, 6940.
[32] C. J. Lin, K. C. Chen, J. L. He, *Wear* **2006**, *261*, 1390.
[33] A. S. Hamdy, M. A. Shoeib, H. Hady, O. F. Abdel Salam, *Surf. Coat. Technol.* **2007**, *202*, 162.
[34] Th. Lampke, A. Leopold, D. Dietrich, G. Alisch, B. Wielage, *Surf. Coat. Technol* **2006**, *201*, 3510.
[35] C. F. Malfatti, J. Z. Ferreira, C. B. Santos, B. V. Souza, E. P. Fallavena, S. Vaillant, J.-P. Bonino, *Corros. Sci.* **2005**, *47*, 567.
[36] Q. Zhao, Y. Liu, E. W. Abel, *Mater. Chem. Phys.* **2004**, *87*, 332.
[37] C. F. Malfatti, H. M. Veit, T. L. Menezes, J. Z. Ferreira, J. S. Rodriguês, J.-P. Bonino, *Surf. Coat. Technol.* **2007**, *201*, 6318.
[38] K. Lu, M. L. Sui, R. Lück, *Nanostr. Mater.* **1994**, *4*, 465.
[39] A. Serebryakov, V. Stelmukh, L. Voropaeva, N. Novokhatskaya, Yu. Levin, A. Gurov, *Nanostr. Mater.* **1994**, *4*, 645.
[40] K. Lu, *Nanostr. Mater.* **1993**, *2*, 643.
[41] H. Habazaki, S.-Q. Ding, A. Kawashima, K. Hashimoto, A. Inoue, T. Masumoto, *Corros. Sci.* **1989**, *29*, 1319.
[42] S. J. Splinter, R. Rofagha, N. S. McIntyre, U. Erb, *Surf. Interface Anal.* **1996**, *24*, 181.
[43] A. Królikowski, P. Butkiewicz, *Electrochim. Acta* **1993**, *38*, 1979.
[44] B. Gillot, K. El Amri, P. Pouderoux, J. P. Bonino, A. Rousset, *J. Alloys Comp.* **1992**, *189*, 151.
[45] F. Bigdeli, S. R. Allahkaram, *Int. J. Mod. Phys.* **2008**, *B 22*, 3031.